Publication Year	2021
Acceptance in OA	2022-03-16T16:56:40Z
Title	The SPHERE infrared survey for exoplanets (SHINE). I. Sample definition and target characterization
Authors	DESIDERA, Silvano, Chauvin, G., Bonavita, M., MESSINA, Sergio, LeCoroller, H., SCHMIDT, TOBIAS MARIUS, GRATTON, Raffaele, Lazzoni, C., Meyer, M., Schlieder, J., Cheetham, A., Hagelberg, J., Bonnefoy, M., Feldt, M., Lagrange, A. -M., Langlois, M., Vigan, A., Tan, T. G., Hambsch, F. -J., Millward, M., ALCALA', JUAN MANUEL, BENATTI, SERENA, Brandner, W., Carson, J., COVINO, Elvira, Delorme, P., D'ORAZI, VALENTINA, Janson, M., RIGLIACO, ELISABETTA, Beuzit, J. -L., Biller, B., Boccaletti, A., Dominik, C., Cantalloube, F., Fontanive, C., Galicher, R., Henning, Th., Lagadec, E., LIGI, ROXANNE, Maire, A. -L., Menard, F., MESA, DINO, Müller, A., Samland, M., Schmid, H. M., Sissa, E., TURATTO, Massimo, Udry, S., Zurlo, A., Asensio-Torres, R., Kopytova, T., Rickman, E., Abe, L., Antichi, J., BARUFFOLO, Andrea, Baudoz, P., Baudrand, J., Blanchard, P., Bazzon, A., Buey, T., Carbillet, M., Carle, M., Charton, J., CASCONE, Enrico, CLAUDI, Riccardo, Costille, A., Deboulbé, A., DE CAPRIO, VINCENZO, Dohlen, K., FANTINEL, Daniela, Feautrier, P., Fusco, T., Gigan, P., GIRO, Enrico, Gisler, D., Gluck, L., Hubin, N., Hugot, E., Jaquet, M., Kasper, M., Madec, F., Magnard, Y., Martinez, P., Maurel, D., Le Mignant, D., Möller-Nilsson, O., Llored, M., Moulin, T., Origné, A., Pavlov, A., Perret, D., Petit, C., Pragt, J., Puget, P., Rabou, P., Ramos, J., Rigal, F., Rochat, S., Roelfsema, R., Rousset, G., Roux, A., SALASNICH, Bernardo, Sauvage, J. -F., Sevin, A., Soenke, C., Stadler, E., Suarez, M., Weber, L., Wildi, F.
Publisher's version (DOI)	10.1051/0004-6361/202038806
Handle	http://hdl.handle.net/20.500.12386/31639
Journal	ASTRONOMY & ASTROPHYSICS
Volume	651

Zuckerman, B., & Song, I. 2004, ARA&A, 42, 685
Zuckerman, B., & Song, I. 2012, ApJ, 758, 77
Zuckerman, B., Rhee, J. H., Song, I., & Bessell, M. S. 2011, ApJ, 732, 61
Zurlo, A., Vigan, A., Galicher, R., et al. 2016, A&A, 587, A57
Zurlo, A., Mesa, D., Desidera, S., et al. 2018, MNRAS, 480, 35

[1] INAF – Osservatorio Astronomico di Padova, Vicolo dell'Osservatorio 5, 35122 Padova, Italy
e-mail: silvano.desidera@oapd.inaf.it
[2] Univ. Grenoble Alpes, CNRS, IPAG, 38000 Grenoble, France
[3] SUPA, Institute for Astronomy, University of Edinburgh, Blackford Hill, Edinburgh EH9 3HJ, UK
[4] Centre for Exoplanet Science, University of Edinburgh, Edinburgh EH9 3HJ, UK
[5] INAF – Osservatorio Astrofisico di Catania, Via S. Sofia 78, 95123, Catania, Italy
[6] Aix Marseille Univ, CNRS, CNES, LAM, Marseille, France
[7] Hamburger Sternwarte, Gojenbergsweg 112, 21029 Hamburg, Germany
[8] LESIA, Observatoire de Paris, Université PSL, CNRS, Sorbonne Université, Université de Paris, 5 place Jules Janssen, 92195 Meudon, France
[9] Dipartimento di Fisica e Astronomia Galileo Galilei, Universitá di Padova, Vicolo dell'Osservatorio 3, 35122, Padova, Italy
[10] Department of Astronomy, University of Michigan, Ann Arbor, MI 48109, USA
[11] Institute for Particle Physics and Astrophysics, ETH Zurich, Wolfgang-Pauli-Strasse 27, 8093 Zurich, Switzerland
[12] Exoplanets and Stellar Astrophysics Laboratory, Code 667, NASA Goddard Space Flight Center, 8800 Greenbelt Rd., Greenbelt, MD 20771, USA
[13] Max Planck Institute for Astronomy, Königstuhl 17, 69117 Heidelberg, Germany
[14] Geneva Observatory, University of Geneva, Chemin des Mailettes 51, 1290 Versoix, Switzerland
[15] CRAL, CNRS, Université Lyon 1, Université de Lyon, ENS, 9 avenue Charles Andre, 69561 Saint Genis Laval, France
[16] Perth Exoplanet Survey Telescope, Western Australia, Australia
[17] Remote Observatory Atacama Desert, Chile
[18] York Creek Observatory, Georgetown, Tasmania, Australia
[19] INAF – Osservatorio Astronomico di Capodimonte, Salita Moiariello 16, 80131 Napoli, Italy
[20] INAF – Osservatorio Astronomico di Palermo, Piazza del Parlamento, 1, 90134 Palermo, Italy
[21] College of Charleston, Department of Physics & Astronomy, 66 George St, Charleston, SC 29424, USA
[22] Department of Astronomy, Stockholm University, 10691 Stockholm, Sweden
[23] Anton Pannekoek Institute for Astronomy, Science Park 9, 1098 XH Amsterdam, The Netherlands
[24] Center for Space and Habitability, University of Bern, 3012 Bern, Switzerland
[25] Université Cote d'Azur, OCA, CNRS, Lagrange, France
[26] INAF – Osservatorio Astronomico di Brera, Via E. Bianchi 46, 23807 Merate, Italy
[27] STAR Institute, University of Liège, Allée du Six Août 19c, 4000 Liège, Belgium
[28] Núcleo de Astronomía, Facultad de Ingeniería y Ciencias, Universidad Diego Portales, Av. Ejercito 441, Santiago, Chile
[29] Escuela de Ingeniería Industrial, Facultad de Ingeniería y Ciencias, Universidad Diego Portales, Av. Ejercito 441, Santiago, Chile
[30] DKFZ, Heidelberg, Germany
[31] Ural Federal University, Yekaterinburg 620002, Russia
[32] INAF – Osservatorio Astrofisico di Arcetri Largo Enrico Fermi 5, 50125 Firenze, Italy
[33] ONERA (Office National dEtudes et de Recherches Arospatiales), B.P.72, 92322 Chatillon, France
[34] European Southern Observatory (ESO), Karl-Schwarzschild-Str. 2, 85748 Garching, Germany
[35] NOVA Optical Infrared Instrumentation Group, Oude Hoogeveensedijk 4, 7991 PD Dwingeloo, The Netherlands

Appendix A: Notes on individual objects

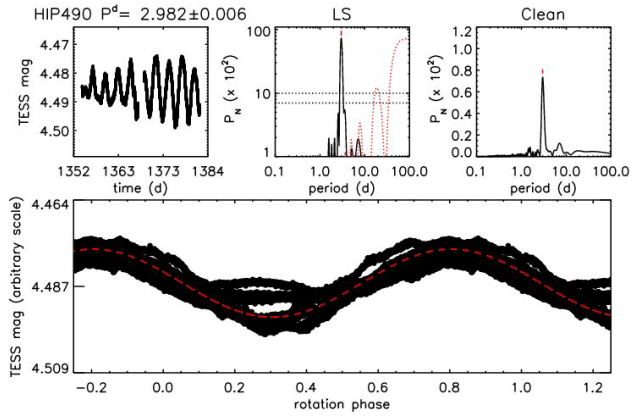

Fig. A.1. Photometric time sequence and periodogram for HIP490 = HD 105.

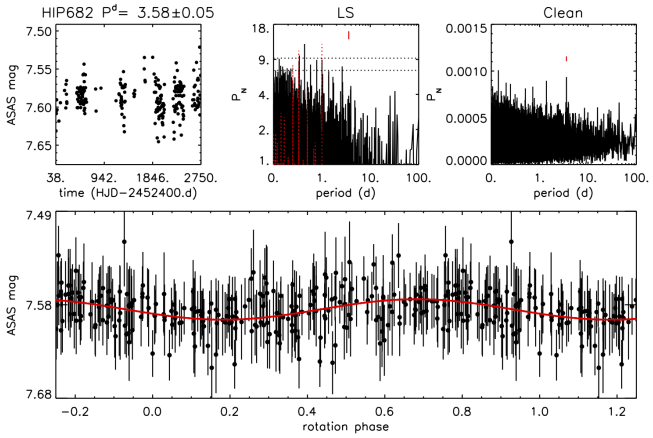

Fig. A.2. Photometric time sequence and periodogram for HIP682 = HD 377.

Together with relevant notes on individual targets, in Figs. A.1–A.85 we summarize the results of our periodogram analysis. In the top left panel we plot magnitudes versus TESS Julian Date, unless differently specified. In the top middle panel we plot the Lomb−Scargle periodogram with the spectral window function (red dotted line) and power level corresponding to FAP = 0.01% and 0.1% (horizontal dashed line), and we indicate the peak corresponding to the rotation period. In the top right panel, we plot the CLEAN periodogram. In the bottom panel we plot the light curve phased with the rotation period. The solid line represents the sinusoidal fit.

HIP 490 = HD 105. We measured for the first time the rotation period from the TESS photometric time series (Fig. A.1). The light curve exhibits a significant evolution of amplitude in subsequent rotation cycles.

HIP 682 = HD 377. Star with resolved debris disk (Choquet et al. 2016). We measured for the first time the rotation period from the All Sky Automated Survey (ASAS) photometric time series (Fig. A.2). This allowed us to refine the age estimate of the target, which results very close to that of the Pleiades. The star does not result as a member of any known young moving group. The inclination estimated from rotation period, $v \sin i$, and stellar radius is compatible within the error with that of the disk ($85 \pm 5°$). It was set as P0 target for disk characterization purposes.

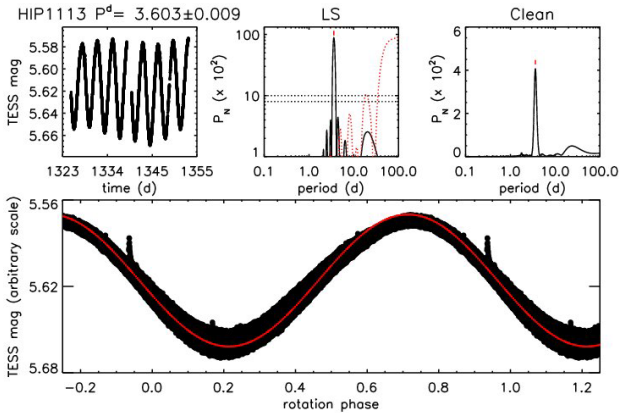

Fig. A.3. Photometric time sequence and periodogram for HIP1113.

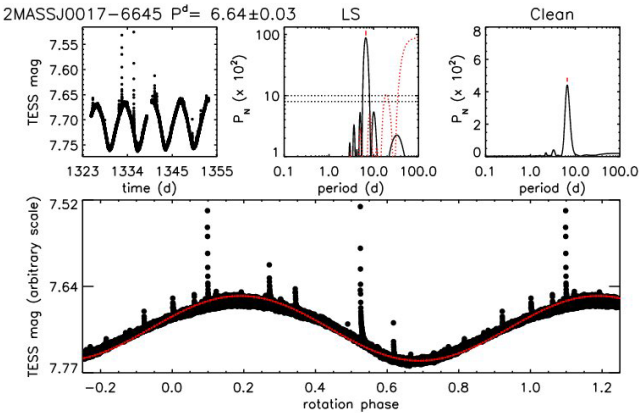

Fig. A.4. Photometric time sequence and periodogram for 2MASSJ0017-6645.

HIP 1113 = HD 987. The photometric rotation period first measured by Messina et al. (2010) is confirmed by our analysis of the TESS data (Fig. A.3). The TESS data revealed one flare event superimposed on a quite stable light curve.

2MASS J00172353-6 645 124. The photometric rotation period first measured by Messina et al. (2017) is confirmed by our analysis of the TESS data (Fig. A.4). The TESS data revealed, superimposed on a quite stable light curve, the presence of multiple flare events, that support the young age estimated for this M-type star.

HIP 1481 = HD 1466. We measured for the first time the rotation period from the TESS photometric time series (Fig. A.5).

HIP 1993 = CT Tuc. The photometric rotation period first measured by Messina et al. (2010) is confirmed by our analysis of the TESS data (Fig. A.6). The TESS data revealed, superimposed on a quite stable light curve, the presence of multiple flare events, that support the young age estimated for this M-type star.

HIP 2578 = HD 3003. Member of Tuc-Hor association. It is comoving with the quadruple system HIP 2484+HIP 2487 (both of which are also visual binaries) at 25 350 au projected separation. Masses of the components in Table 10 taken from Tokovinin (2008).

HIP 6276 = BD-12 243. We measured for the first time the rotation period from the TESS photometric time series (Fig. A.7), which is in rough agreement with the earlier measurement ($P = 6.40$ d) by Wright et al. (2011). TESS data revealed, superimposed on a quite stable light curve, the presence of multiple flare events.

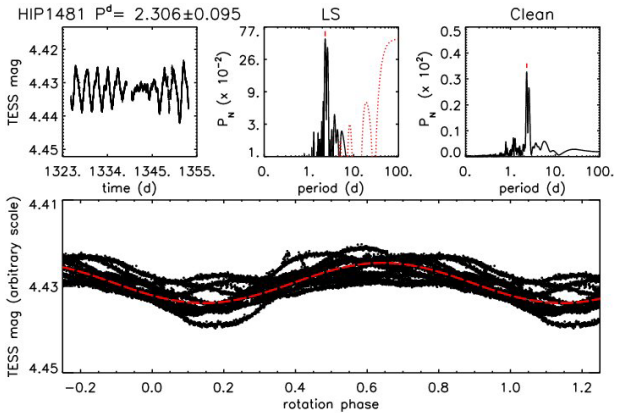

Fig. A.5. Photometric time sequence and periodogram for HIP1481.

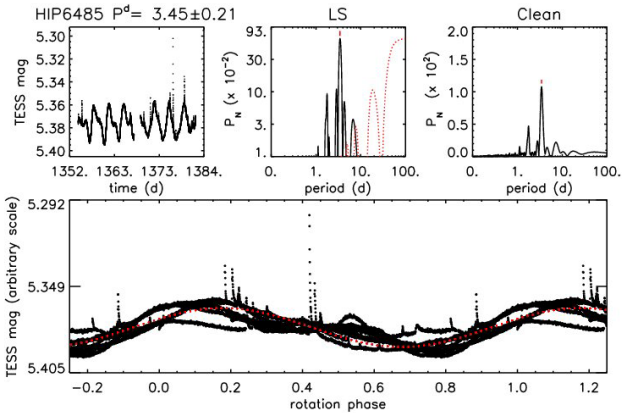

Fig. A.8. Photometric time sequence and periodogram for HIP6485.

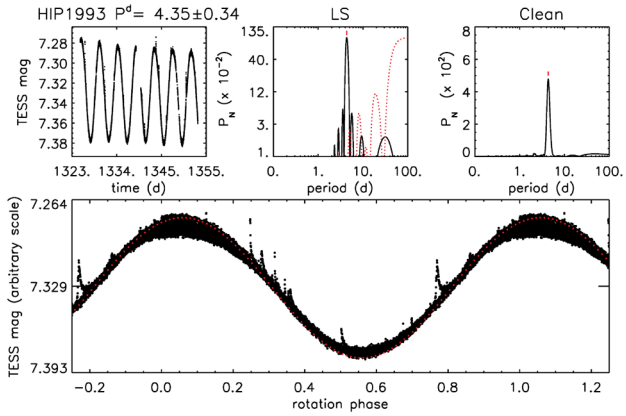

Fig. A.6. Photometric time sequence and periodogram for HIP1993.

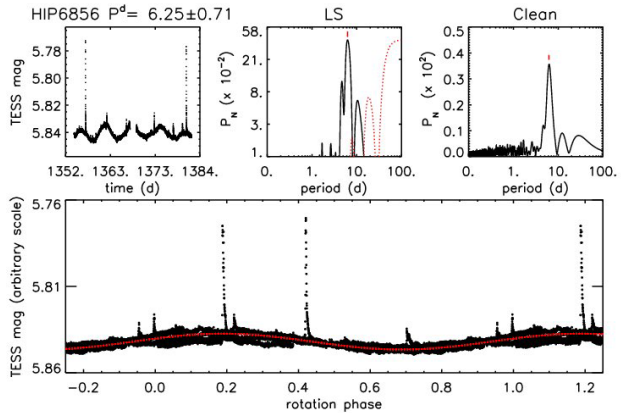

Fig. A.9. Photometric time sequence and periodogram for HIP6856.

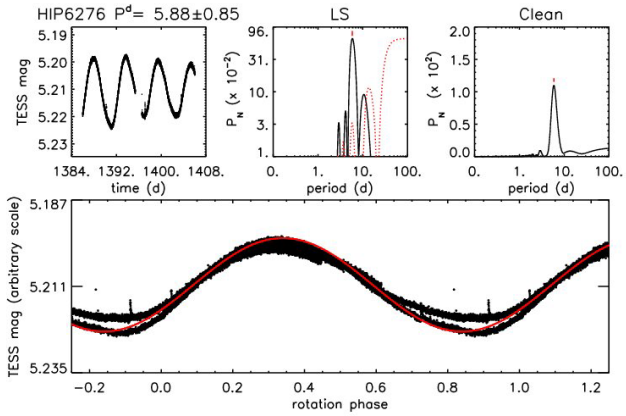

Fig. A.7. Photometric time sequence and periodogram for HIP6276.

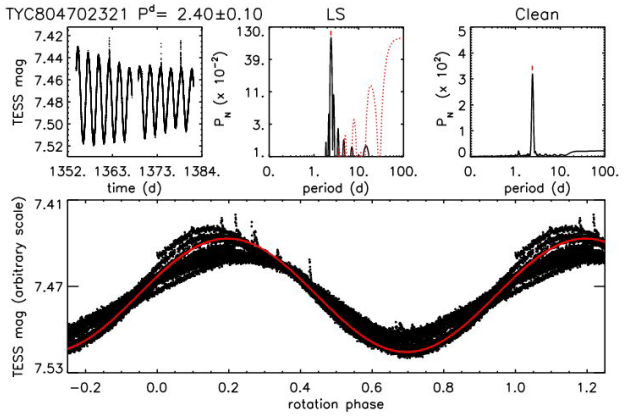

Fig. A.10. Photometric time sequence and periodogram for TYC 8047-0232-1.

HIP 6485 = HD 8558. The photometric rotation period first measured by Messina et al. (2010) is confirmed by the TESS data (Fig. A.8) and is in agreement with the measurements by Oelkers et al. (2018). TESS data reveal significant evolution of light curve amplitude and numerous flare events.

HIP 6856 = HD 9054. We measured for the first time the rotation period from the TESS photometric time series (Fig. A.9), which revealed numerous flare events.

TYC 8047-0232-1. Star with brown dwarf companion discovered by Chauvin et al. (2005a). The photometric rotation period first measured by Messina et al. (2010) is confirmed by our analysis of the TESS data (Fig. A.10).

HIP 11360 = HD 15115. The revised RV from Desidera et al. (2015) supports the membership to the Tuc-Hor association (93.7% using BANYAN). The star has a spatially resolved edge-on debris disk (Kalas et al. 2007; Engler et al. 2019). We measured for the first time the rotation period from the TESS photometric time series (Fig. A.11).

HIP 13402 = HD 17925 = EP Eri. Flagged as RS CVn variable, with spectral types K1+K2 and period 6.85 days in Rodriguez et al. (2015). However, HARPS observations available in ESO archive allow us to rule out the presence of close stellar companions (rms = 28 m s^{-1} from 42 RVs over

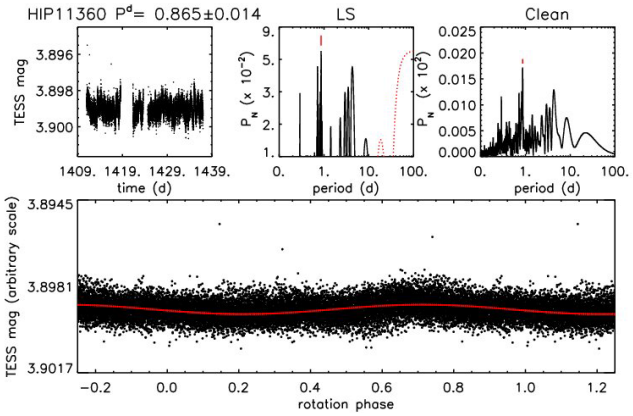

Fig. A.11. Photometric time sequence and periodogram for HIP11360.

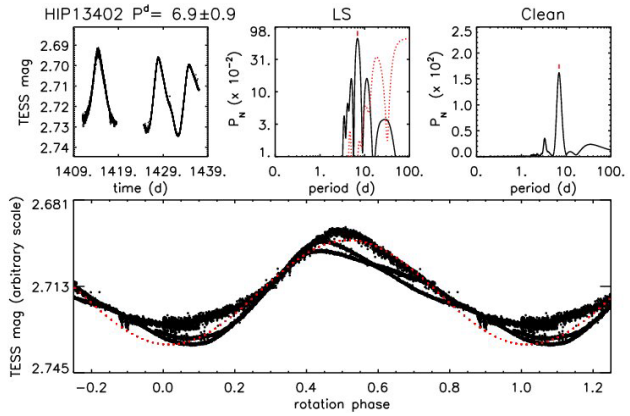

Fig. A.12. Photometric time sequence and periodogram for HIP13402.

1200 days). We then kept the star in the sample. The photometric rotation period first measured by Messina et al. (2001) is confirmed by our analysis of the TESS data (Fig. A.12).

HIP 14551 = HD 19545. Originally classified as a member of Tuc-Hor (Zuckerman et al. 2011), the updated analysis indicates membership in the Columba association. The wide companion, UCAC4 311-003056, has been also classified as a member of the Columba association (Gagné et al. 2018b). The small but formally significant differences in parallax and proper motion make it possible that the two stars do not form a true binary system and are only projected very close on the sky (59 arcsec).

TYC 7026-0325-1. The photometric rotation period first measured by Messina et al. (2010) is confirmed by our analysis of the TESS data (Fig. A.13).

HIP 15457 = HD 20630 = κ Cet. The photometric rotation period first measured by Messina et al. (2001) is confirmed by our analysis of the TESS data (Fig. A.14). The presence of numerous flare events are detected.

TYC 8060-1673-1. The photometric rotation period first measured by Messina et al. (2010) is confirmed by our analysis of the TESS data (Fig. A.15).

HIP 17764 = HD 24636. We measured for the first time the rotation period from the TESS photometric time series (Fig. A.16).

HD 25284B. We measured for the first time the rotation period from the TESS photometric time series (Fig. A.17). We note that according to SIMBAD coordinates, HD 25284A and B are unresolved in the TESS photometry. As shown in the

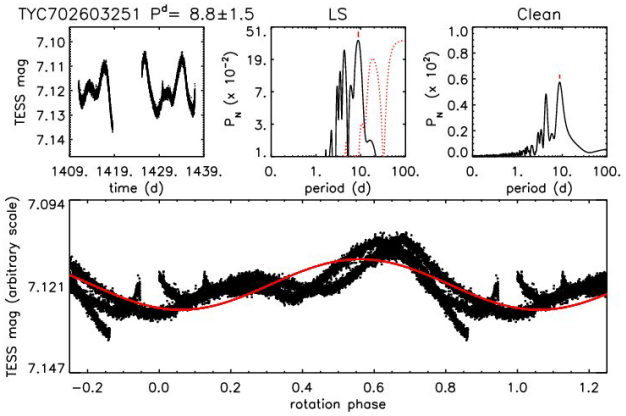

Fig. A.13. Photometric time sequence and periodogram for TYC 7026-0325-1.

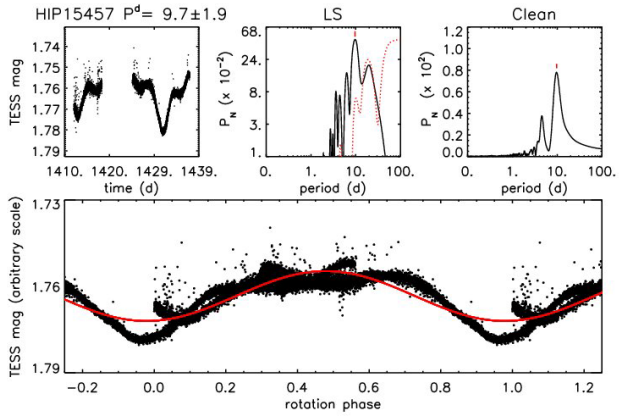

Fig. A.14. Photometric time sequence and periodogram for HIP15457 (κ Cet).

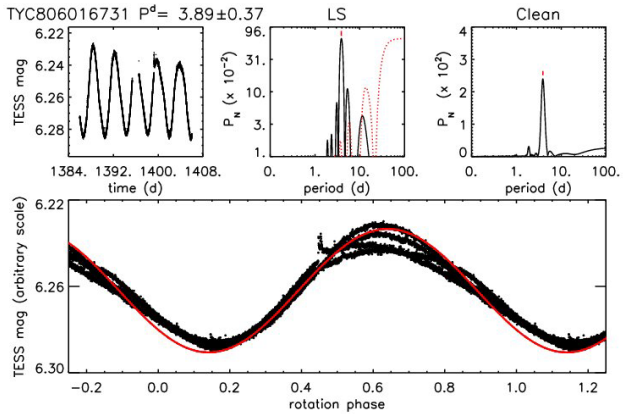

Fig. A.15. Photometric time sequence and periodogram for TYC 8060-1673-1.

figure, both Lomb–Scargle and Clean detected three significant periods that are in order of decreasing power $P = 4.54$ d, $P = 2.26$ d, and $P = 0.31$ d. Considering that HD 25284B has $v \sin i = 6.9\,\mathrm{km\,s^{-1}}$, its rotation period should be $P = 4.54$ days to reconcile with stellar radius and projected rotational velocity. Following similar reasoning, considering that HD 25284A has $v \sin i = 69.8\,\mathrm{km\,s^{-1}}$, its rotation period should be $P = 0.31$ d. The remaining period $P = 2.26$ d, half of the primary period, may arise from the double-dip shape of the light curve.

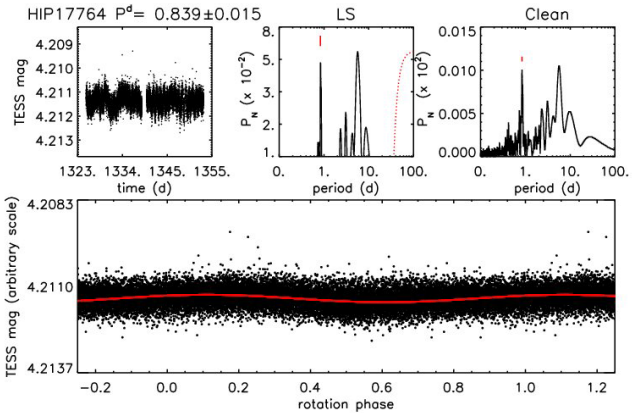

Fig. A.16. Photometric time sequence and periodogram for HIP17764.

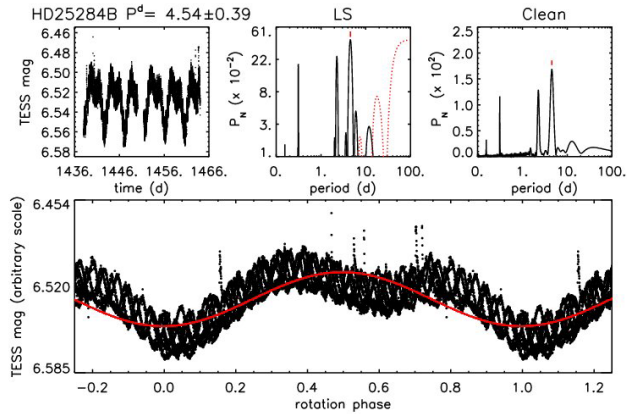

Fig. A.17. Photometric time sequence and periodogram for HD25284B.

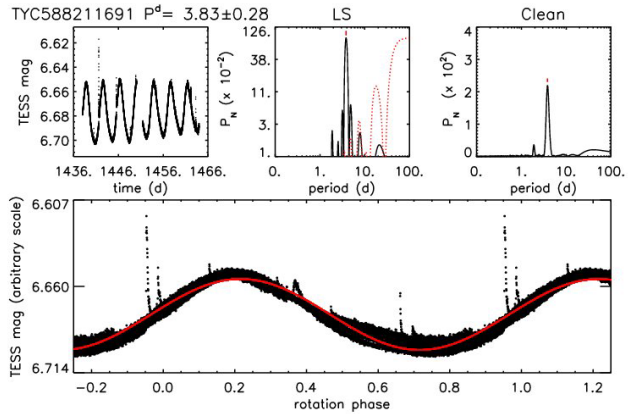

Fig. A.18. Photometric time sequence and periodogram for TYC 5882-1169-1.

TYC 5882-1169-1 = BD-15 705. Originally classified as a member of the Columba association, the updated analysis indicates membership in the Tuc-Hor association. The photometric rotation period first measured by Messina et al. (2010) is confirmed by our analysis of the TESS data (Fig. A.18). More flare events are detected in the TESS time series.

51 Eri = HIP 21547. The star has a planetary companion discovered by Macintosh et al. (2015). The periodogram analysis of the TESS data shows evidence of multi-periodicity with the most powerful peak at $P = 1.84 \pm 0.06$ days and the secondary power peak in agreement with the early rotation period measurement by Koen & Eyer (2002) (Fig. A.19–A.21).

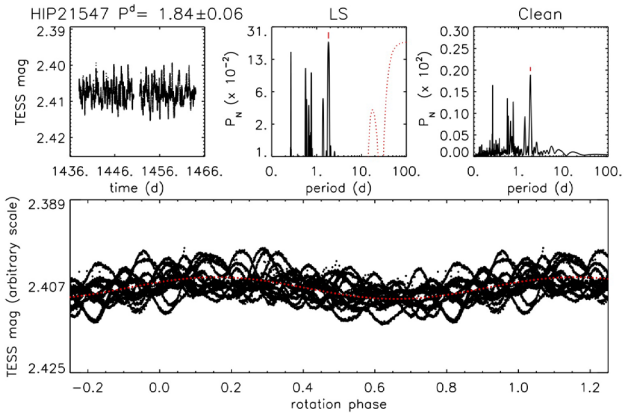

Fig. A.19. Photometric time sequence and periodogram for 51 Eri (HIP21547).

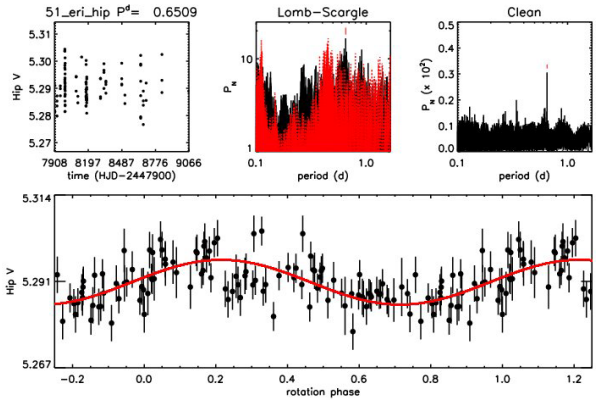

Fig. A.20. Photometric time sequence and periodogram for 51 Eri (HIP21547) (from HIPPARCOS).

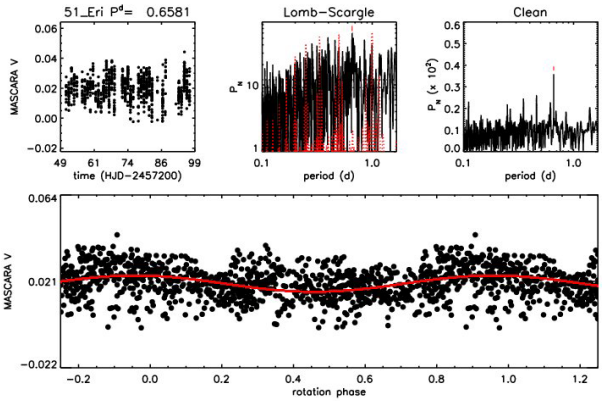

Fig. A.21. Photometric time sequence and periodogram for 51 Eri (HIP 21547) (from the Mascara survey).

Considering the F0IV spectral type, it is likely that most periodicities arise from pulsations rather than variability induced by undiscovered close companions.

HIP 22226 = HD 30447. Star with debris disk spatially resolved by Soummer et al. (2014). The star has a close pair of faint comoving companions with very similar astrometric parameters at 622″ = 50 100 au projected separation (*Gaia* DR2 4881308710762664576 and *Gaia* DR2 4881308710764495744, unique entry in 2MASS, 2MASS J04463413-2 627 559, $\Delta G = 0.15$ mag). The very wide separation is larger than the typical limit for binaries. These objects